#### REPORT



# Bio-optical signatures of in situ photosymbionts predict bleaching severity prior to thermal stress in the Caribbean coral species *Acropora palmata*

Kenneth D. Hoadley $^{1,2}$   $\odot$  · Sean Lowry $^{1,2}$  · Audrey McQuagge $^{1,2}$  · Shannon Dalessandri $^{1,2}$  · Grant Lockridge $^{2,6}$  · Sibelle O'Donnell $^4$  · Holland Elder $^4$  · Maria Ruggeri $^4$  · Eleftherios Karabelas $^5$  · Courtney Klepac $^{3,5}$   $\odot$  · Carly Kenkel $^4$   $\odot$  · Erinn M. Muller $^{3,5}$   $\odot$ 

Received: 13 July 2023 / Accepted: 14 December 2023 / Published online: 18 January 2024 © The Author(s), under exclusive licence to International Coral Reef Society (ICRS) 2024

**Abstract** The identification of bleaching tolerant traits among individual corals is a major focus for many restoration and conservation initiatives but often relies on large scale or high-throughput experimental manipulations which may not be accessible to many front-line restoration practitioners. Here, we evaluate a machine learning technique to generate a predictive model which estimates bleaching severity using non-destructive chlorophyll-a fluorescence photo-physiological metrics measured with a low-cost and open access bio-optical tool. First, a 4-week long thermal bleaching experiment was performed on 156 genotypes of Acropora palmata at a land-based restoration facility. Resulting bleaching responses (percent change in Fv/Fm or Absorbance) significantly differed across the four distinct light-response phenotypes (clusters) generated via a photo-physiology-based dendrogram, indicating strong concordance between fluorescence-based photo-physiological metrics and future bleaching severity. The proportion of thermally tolerant Clade D symbionts also differed significantly across photo-physiology-based dendrogram clusters,

**Supplementary Information** The online version contains supplementary material available at https://doi.org/10.1007/s00338-023-02458-5.

- Kenneth D. Hoadley kdhoadley@ua.edu
- University of Alabama, Tuscaloosa, AL, USA
- <sup>2</sup> Dauphin Island Sea Lab, Dauphin Island, AL, USA
- Mote Marine Laboratory, Sarasota, FL, USA
- Department of Biological Sciences, University of Southern California, 3616 Trousdale Parkway, Los Angeles, CA 90089, USA
- Mote Marine Laboratory, Summerland Key, FL, USA
- <sup>6</sup> US Naval Research Laboratory, Stennis, MS 39426, USA

linking light-response phenotypes and bleaching response with underlying symbiont species. Next, these correlations were used to train and then test a Random Forest algorithm-based model using a bootstrap resampling technique. Correlation between predicted and actual bleaching responses in test corals was significant (p < 0.0001) and increased with the number of corals used in model training (Peak average  $R^2$  values of 0.45 and 0.35 for Fv/Fm and absorbance, respectively). Strong concordance between photo-physiology-based phenotypes and future bleaching severity may provide a highly scalable means for assessing reef corals.

 $\begin{tabular}{ll} \textbf{Keywords} & Coral bleaching} \cdot Coral photosymbiont \\ phenotyping \cdot Symbiodiniaceae photobiology \cdot Bio-optical \\ bleaching prediction \cdot High-throughput trait selection \\ \end{tabular}$ 

### Introduction

Increasingly frequent coral bleaching events caused by ocean warming continue to decimate reef systems across the globe (Hughes et al. 2017, 2018). More than ever before, coral reef restoration initiatives are focused on combating ecosystem loss through the transplant of coral fragments onto impacted sites (Boström-Einarsson et al. 2020; Caruso et al. 2021; Voolstra et al. 2021). Such efforts are meant to mitigate further ecosystem decline while more permanent solutions to ocean warming can be found. The success of many coral restoration initiatives, especially those on heavily impacted sites or areas expected to experience severe environmental perturbations, is reliant on establishing colonies with more environmentally resilient traits (Voolstra et al. 2020, 2021; Grummer et al. 2022; Klepac et al. 2023). Indeed, high phenotypic variability in bleaching severity to thermal stress exists within and across individual coral colonies



(Parkinson et al. 2015; Kenkel and Matz 2016), and environments (Kenkel et al. 2013b; Palumbi et al. 2014; Barshis et al. 2018; Voolstra et al. 2020) and likely reflects the outcome of various host and/or symbiont metabolic or cellular pathways which together regulate the expulsion of symbiont cells (coral bleaching) from the host tissue (Weis 2008). However, initial identification of reef systems or individual coral colonies with desirable traits such as thermal resilience is challenging (Parkinson et al. 2020), often requiring expensive and time-consuming efforts not available to most front-line restoration practitioners. Additionally, experimental exposures frequently require sacrificing coral fragments for research purposes, activities that require having excess biomass of already rare coral species and genotypes, which is becoming more difficult for groups to accommodate especially for critically endangered coral species. New tools are needed that utilize our collective knowledge of coral physiology and/or genetics to inform on key traits and facilitate colony selection for restoration activities without the need for sacrificing precious coral biomass.

The intracellular symbiotic algae (family: Symbiodiniaceae) are typified by high genetic variability within and across individual species (LaJeunesse et al. 2018). Our understanding of phenotypic variability across these algal species lags behind the genetics, largely due to challenges in measuring cellular characteristics of algae living within the host tissue. Nevertheless, coral thermal tolerance is often tied to specific symbiont species (Abrego et al. 2008; Suggett et al. 2017; van Woesik et al. 2022) and further consideration is needed for how functional traits link to underlying genetic variability across this algal lineage. Bio-optical tools such as the Pulse Amplitude Modulated (PAM) fluorometer that measures algal-specific traits such as variable chlorophyll a fluorescence have already provided critical insight into the variability of thermal resilience across coral species, and individual colonies (Warner et al. 1999; Voolstra et al. 2020; Cunning et al. 2021). However, more sophisticated fast repetition rate fluorometers can offer greater insight into algal-centric thermal responses (Hoadley et al. 2019, 2021) or functional trait variability (Suggett et al. 2015, 2022), leading the way toward further integration of these tools for coral research. Recently, we developed a low-cost, multispectral, and fast repetition rate fluorometer (FRRf) capable of generating over 1000 individual metrics within a short (11-min) timespan and showcased its utility in defining photosynthetic phenotypes across algal genera hosted by seven different coral species under active restoration in the Florida Keys (Hoadley et al. 2023). Importantly, this work and others suggest that algal-centric photo-physiological metrics are correlated with bleaching severity and such information could provide a scalable means for identifying individual colonies, coral species, or reef sites with high tolerance to thermal stress or other desirable traits. However, further exploration is needed to understand if these highly dimensional and algal-centric physiological metrics, along with machine learning techniques can be effectively utilized to develop predictive models for accurate trait-based selection of reef corals.

Here, we evaluate the use of a machine learning technique to generate a predictive model which estimates bleaching tolerance based solely on rapid and non-destructive chlorophyll-a fluorescence, photo-physiological metrics measured with a low-cost and open access bio-optical tool. First, fluorescence-based phenotypes were measured on 156 genotypes (genets) of Acropora palmata using bio-optical tools that assess algal photo-physiological metrics. This was followed by a 4-week long thermal bleaching experiment performed on all genets at a land-based restoration facility in the Florida Keys. Next, correlations between algal photo-physiological metrics and bleaching response (percent change in Fv/Fm or Absorbance at 675 nm) were ranked and corals were randomly selected for use in model training or testing. Evaluation was performed using a bootstrap technique to ensure robust model performance across all coral genotypes. Prior studies that have used host genetic information for predicting thermal tolerance found that accuracy improved dramatically when environmental or information on the dominant symbiont type were also incorporated into their model (Fuller et al. 2020). Our study extends this predictive concept by focusing on the underlying phenotype of the symbiont as a tool for assessing coral tolerance. Artificial intelligence-based techniques are increasingly applied within conservation and earth sciences (Evans et al. 2012; Reichstein et al. 2019) and our study demonstrates its utility for trait-based selection of reef corals using low-cost and rapid, bio-optical measurements of symbiont physiology.

#### Materials and methods

## Coral selection and husbandry

Mote's International Center for Coral Reef Research and Restoration (MML-IC2R3) on Summerland Key, Florida contains approximately 60 land-based raceways, supplied with filtered, UV sterilized, temperature-controlled, near-shore seawater and maintained underneath 60% shade cloth canopies and corrugated clear-plastic rain guards as needed. Peak midday irradiance within these outdoor raceway aquaria was measured (Walz, 4pi sensor) in 2021 (Hoadley et al. 2023) at ~400 μmol m<sup>-2</sup> s<sup>-1</sup> under full sunlight, in the month of May. Individual coral genotypes were pulled from Mote's restoration broodstock, with fragments mounted to ceramic disks (Boston Aqua Farms, 3 cm diameter) using cyanoacrylate gel (Bulk Reef Supply). Of the 156 *A. palmata* within the study, 30 were reared as sexual recruits from



a batch cross collected from the Upper Florida Keys in 2013 (29 genets) and 2015 (1 genet), 80 genets were the product of a batch cross sourced from Elbow/Biscayne in 2017, 42 genets were the product of a batch cross sourced from the lower keys in 2020, and 4 were sourced as collections directly from Looe Key, Sand Key, and Turtle reef in 2018, 2021, 2021, and 2014, respectively. Genotype identification was confirmed using single nucleotide polymorphism loci (Kitchen et al. 2020). All coral fragments utilized in this study had been propagated in Mote's ex-situ nursery and acclimated to the Climate and Acidification Ocean Simulator (CAOS) system for 4 weeks prior to the start of experimental conditions.

# Phenotyping coral photosymbionts using chlorophyll $\boldsymbol{a}$ fluorescence

Prior to experimental bleaching, phenotypic measurements were derived using FRRf (between March 31st and April 5th, 2022) from a single coral fragment (ramet) per A. palmata genotype. Each fragment was dark acclimated for 20 min prior to fluorescence measurements. All measurements were taken between roughly 2-8 h after sunrise. Importantly, the fragment used for capturing phenotypic data is separate from the two fragments used to assess bleaching response metrics at the end of the experiment. Within-colony physiological variability is common across coral species due to differences in their microclimate (light, water flow, inter-species interactions), and is thus a serious consideration when evaluating physiology. While Hoadley et al. (2023) and McQuagge et al. (2023) both show ramets from the same colony tend to cluster together within the same light-response phenotype when measured using our FRRf protocol, results can vary across species. Phenotyping and bleaching multiple fragments per colony would be ideal for assessing colony response but goes beyond the scope of this study. Nevertheless, the use of three separate fragments colony<sup>-1</sup> in this study allows for some intra-colony variability to be incorporated into our predictive design.

Fluorescence excitation in our phenotyping protocol was achieved using four excitation wavelengths (415, 448, 470 and 505 nm) which preferentially target different photopigments within the symbiotic algae. Fluorescence induction, which consists of the lowest initial fluorescent measurement ( $F_0$ ) to maximal fluorescence where the signal appears to plateau (Fm) consisted of a series of brief excitation pulses, each 1.3-µs long and followed by a 3.4-µs dark interval. For our samples, 32 flashlets was sufficient to reach a plateau in our induction curve which was then used to calculate spectrally dependent  $F_0$  and Fm values, along with subsequent metrics (( $\Phi$ PSII, NPQ, and qP) as previously described in Hoadley et al. (2023)). Additionally, spectrally dependent

excitation pressure over PSII ( $Q_{\rm m}$ ) was also calculated using the equation:

$$Q_{\rm m} = 1 - \left(\frac{\text{quantum yield}}{\text{maximum quantum yield}}\right)$$

The excitation pressure over PSII equation is adapted from (Iglesias-Prieto et al. 2004) where maximum quantum yield reflects the highest quantum yield value within the actinic light protocol for a given sample and excitation wavelength. Power (irradiance in PAR) estimates were used to determine the spectrally dependent functional absorption cross section of PSII ( $\sigma_{PSII}$ ) and antennae bed quenching (ABQ) according to previously published methods (Kolber et al. 1998; Oxborough et al. 2012). A 300-ms fluorescent relaxation measurement followed immediately after induction and utilized the same 1.3-µs excitation flash but followed by an exponentially increasing dark period (starting with 59- $\mu$ s). This induction and relaxation process was run sequentially for each excitation color with a 200-ms delay in between each run. Measured values reflect an average of 6 repeats per sampling time point. Fluorescent measurements were acquired during a 6-min actinic light protocol which began with an initial dark period, followed by three different light intensities (200, 50, 400 µmol m<sup>-2</sup> s<sup>-1</sup>) and a dark recovery period (See PAR profile in Fig. 1). A total of 28 evenly spaced sampling time points were recorded during this actinic light protocol. Definitions and units for each of our 8 spectrally dependent photo-physiological metrics calculated for each sampling time point in our phenotyping protocol can be reviewed in Table 1.

### Thermal bleaching experiment

Using the Climate and Acidification Ocean Simulator (CAOS) system located at MML-IC2R3, a four-week long thermal bleaching experiment was performed on the coral species, Acropora palmata (n = 156 genotypes) from April 2 to May 6, 2022. All coral fragments utilized in this study were acclimated for 1 month within the CAOS system prior to the start of the experimental treatment. Control and heat treatments consisted of three shallow raceways per treatment; however, only a single fragment from one control and one high-temperature raceway was utilized in the present study. Filtered seawater was continuously supplied to each raceway (118 L hr<sup>-1</sup>), with recirculating flow provided by a 5679 L hr<sup>-1</sup> external pump to supply the heat exchange system. Additional circulation was provided by four submersible pumps (454 L hr<sup>-1</sup>, Dwyer). All experimental systems were maintained underneath 60% shade cloth canopies and clear plastic rain guards. Experimental systems experienced similar light levels as described above (~400 µmol m<sup>-2</sup> s<sup>-1</sup> peak midday sunlight). At the start of the experiment (April



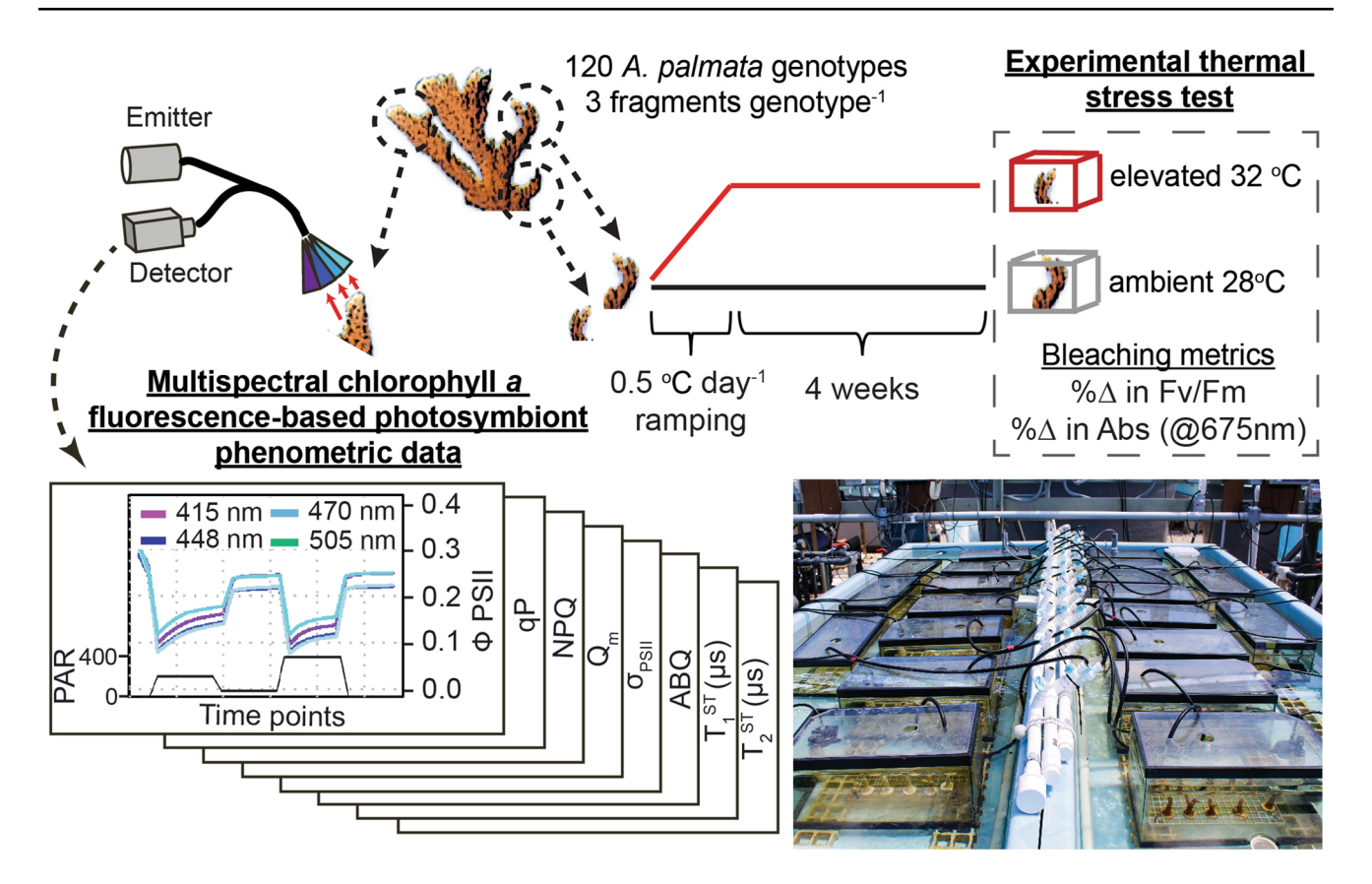


**Fig. 1** Experimental Setup: For each *Acropora palmata* colony, three fragments were removed for use in the experiment. Chlorophyll-a fluorescence-based measurements were recorded from one fragment using a single turnover, multispectral fluorometer. Bottom left graphs reflect the multispectral data and actinic light protocol used in our analysis. The other two fragments were placed into control and treatment tanks and exposed to a four-week-long thermal experiment. At

the end of the thermal experiment, Fv/Fm and Absorbance readings were measured from the two fragments (control and treatment) and utilized to calculate the  $\%\Delta$  in response to high temperature. Bottom right photograph reflects the experimental bleaching raceways and tanks used in the study (corals in photograph are *A. cervicornis* and not part of this work)

Table 1 Table of photo-physiological parameters: Each defined parameter is represented by spectrally dependent values at each sampling time point (Fig. 1)

Term	Definition	Units
$\Phi_{ m PSII}$	Quantum yield of PSII. Measures the proportion of light energy captured by chlorophyll which is then utilized by the PSII reaction center for photosynthesis	No units
qP	Photochemical quenching. Fraction of PSII reaction centers able to utilize light energy for photosynthesis	No units
NPQ	Non-photochemical quenching. Light energy dissipation pathway describing the downregulation of PSII	No units
$\sigma_{ m PSII}$	Absorption cross section of PSII. A measure of photon capture by light-harvesting compounds connected to a PSII reaction center	$nm^2$
ABQ	Antennae Bed Quenching, Light energy dissipation pathway involving reorientation of light-harvesting compounds	No units
$Q_{\mathrm{m}}$	Excitation pressure over PSII	No units
${ au_1}^{ ext{ST}}$	Rate constant for reoxidation of the Qa site of the D1 protein within the PSII reaction center	$\mu$ -seconds
$ au_2^{ ext{ST}}$	Rate constant for reoxidation within and downstream of the plastoquinone pool	$\mu$ -seconds

2, 2022), the high-temperature raceway increased from 27.5 to 31.5 °C by 0.5 °C each day (8 days total). Control raceways remained at 27.5 °C C for the duration of the 1-month experiment and high-temperature raceways remained at

31.5 °C for 3 weeks and 32.0 °C for the remainder of the 1-month experiment (~13 DHW total). This final 0.5 °C increase was done to further induce bleaching response within corals. It is worth mentioning that 0.5 °C per day is



(from an environmental perspective) a relatively fast change in average temperature and results may have differed using a slower ramping rate.

# Genera level Symbiodiniaceae relative abundance determination

While initial phenotyping was done in late March-early April, all ramets were snap frozen in LN<sub>2</sub> for genotyping at the end of the experiment (May 6-7). The data depicted here are from control systems where temperatures remained constant. However, changes in symbiont community may nevertheless have occurred over the 4 week period. Except for four colonies (where a different control ramet from the same colony was used), all DNA extracts are from the same ramet used for initial phenotyping. Holobiont DNA was extracted from snap frozen tissue samples following a modified CTAB-choloroform protocol (Cunning et al. 2016). 20 ng of DNA per was used to quantify symbiont:host (S:H) cell ratios (a metric of symbiont density) via qPCR following Cunning and Baker (2013). A TaqMan (Thermo Fisher Scientific) multiplex assay was used to amplify *Cladoco*pium and Durusdinium actin genes via qPCR (Cunning and Baker 2013). Briefly, duplicate reactions were carried out for each sample using 20 ng template in a 25 µl reaction volume with final concentrations of 100 nM per probe, 50 nM forward primer, and 75 nM reverse primer per primer set. A separate TaqMan master mix was used for Symbiodinuium following (Palacio-Castro et al. 2021) again with duplicate reactions per sample using 20 ng template per reaction in a 25 µl total volume with final concentrations of 300 nM probe, 300 nM Aact forward primer, and 200 nM Aact reverse primer. Host DNA concentrations were quantified using 20 ng of template in duplicate 25 µl reactions using calmodulin gene (CaM) primers at 200 nM final concentration in SYBR-Green assays following (Palacio-Castro et al. 2021). All reactions were adapted for use on the Agilent AriaMX system.

Cycle threshold (CT) values generated from qPCR runs were used to calculate symbiont:host cell ratios. CT values for TaqMan assays were adjusted for differences in fluorescence intensity based on Cunning and Baker (2013). Calculations for relative symbiont to host ratios were completed following the equation from Cunning and Baker (2013). Target copy numbers used in this study were based on Palacio-Castro et al. (2021).

### Bleaching response metrics

Measurements of the maximum quantum yield (Fv/Fm) using 448 nm excitation and absorbance spectra were measured from all experimental fragments on experimental days 39–42 (May 7–8th and 9-10th of 2022 for high temperature

and control treatment groups, respectively). Maximum quantum yield measurements were derived from control and high-temperature fragments after a 20-min dark acclimation period and using the same induction and relaxation protocol described above. Absorption-based measurements were calculated on all coral fragments and achieved by measuring the reflectance spectra according to previously established methods (Rodriguez-Román et al. 2006). A custom fiber optic cable (Berkshire Photonics) coupled a white LED (Luxeon) to a USB2000 spectrophotometer (Ocean Optics) for assessing spectral reflectance from all coral fragments in control and treatment conditions. Reflectance measurements were normalized to a bleached A. palmata skeleton and then converted into absorbance measurements which can serve as a non-invasive proxy for changes in cell density/chlorophyll a content associated with coral bleaching (Rodriguez-Román et al. 2006; Hoadley et al. 2016). Here, absorbance readings were measured at 675 nm which reflects the maximum chlorophyll-a absorbance band.

# Statistical analysis and bleaching response model generation

All analyses were conducted in R (v.3.5.1) (Team 2017). For each coral genotype, bleaching response metrics (Fv/Fm and absorbance at 675 nm) were calculated as the percent change between control and high-temperature fragments (Fig. 2). To minimize bias associated with high correlation between certain photo-physiological traits, a correlation matrix was first used to identify and then remove individual metrics with high correlation (Rho > 0.99) to one another. All remaining photo-physiological metrics were then used to build a phenotypic dendrogram using the R packages pvclust (Suzuki and Shimodaira 2013) and dendextend (Galili 2015). Resulting dendrogram with 10,000 bootstrap iterations was then used to cluster individual genotypes into four distinct clusters/ phenotypes. Next, significant differences across our clusterbased phenotypes for thermally-induced changes in absorbance and Fv/Fm were measured using a one-way ANOVA with a Tukey post hoc (all data fit assumptions of normality). The average proportion of clade D symbionts within colony ramets in each cluster-based phenotype were found to not fit the assumptions of normality (Shapiro-Wilks) and significance was thus assessed using a pairwise Wilcoxon test with Bonferroni correction.

For each photo-physiological metric, a repeated measures linear mixed model with Tukey post hoc (with Bonferroni correction) was used to identify significant differences between identified light-response phenotypes (with colony, light step and excitation color as nested factors) using the lmerTest (Kuznetsova et al. 2017) and multicomp (Hothorn et al. 2008) packages in R.



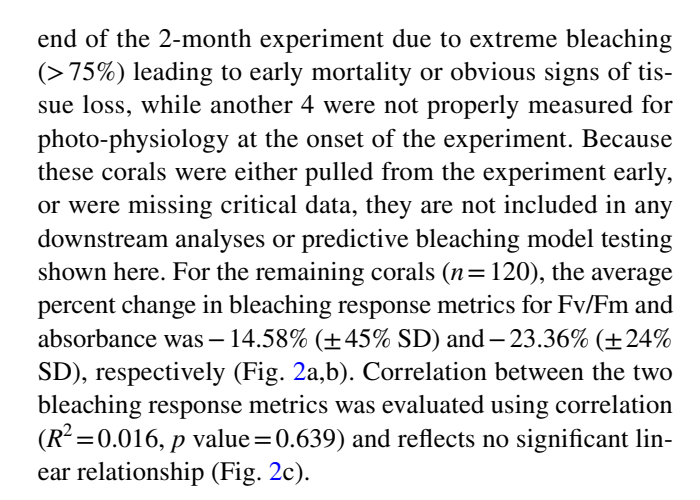
For assessing individual photo-physiological metrics and their correlation to bleaching response, all photo-physiological parameters were first screened for correlation with one another (autocorrelation scores < 0.85 Rho) and then individually tested for correlation (spearman) with bleaching response metrics (% change in absorbance and Fv/Fm). Only photo-physiological metrics with significant (p < 0.05) correlation were included in Fig. 4 (and Supplementary Tables S1 and S2).

Selecting which photo-physiological metrics to use to optimize a predictive bleaching model is a critical step in our analytical pipeline. First, we screened for autocorrelation between photo-physiological metrics. Different correlation cutoff values were used when selecting metrics for the assessment of % change in absorbance (Rho>0.85) and Fv/Fm (Rho>0.75) and are based on resulting predictive performance. Next the Boruta R package (Kursa and Rudnicki 2010) was used to carryout feature selection on the remaining photo-physiological metrics using a random forest-based assessment and prioritization. Resulting prioritized photo-physiological metrics were then used to develop separate models for predicting percent change in Fv/Fm and absorbance (at 675 nm) between control and treatment fragments. Randomly selected coral genotypes were used in model training which consisted of using the Random Forest (RF) regression algorithm to generate each model iteration. The strength of each individual RF model was then tested by predicting bleaching response on 40 randomly selected colonies which were not used to generate the model. Accuracy of each model was then measured using goodness of fit  $(R^2)$  and the root mean square error (RMSE—describes the model error) between predicted and observed bleaching responses (% change in Fv/Fm or absorbance). In addition to goodness of fit, the 40 'test' corals were also ranked based on model predictions, and then the significance of actual bleaching responses between the top and bottom 10 corals was statistically compared using a t test (Fig. 4c,f). Accuracy or our RF models was evaluated as a function of the number of corals (between 20 and 80) used for training, with each model repeated 100 times with randomly selected corals (Bootstrap resampling technique). Importantly, outcomes were always tested using 40 different corals (also randomly selected and separate from those used in training). Bootstrap model scores enable us to evaluate stability and ensure performance was not biased through inclusion/exclusion of a given coral genotype. Raw data along with analytical scripts for generating Figs. 2, 3, 4 and 5 are available via github (khoadley/ bleaching-prediction-2023).

### Results

#### Bleaching response

Of the 156 A. palmata colonies that were evaluated for thermal stress resilience, 32 were removed prior to the



# Linking light-response phenotypes with underlying symbiont type and bleaching response

Our photo-physiology-based dendrogram separated our 120 coral colonies into four distinct clusters with high bootstrap support (Fig. 3a). We then used quantitative PCR to calculate the relative proportion of Clade D in each coral colony, maintained under ambient conditions. The average relative proportion of clade D for phenotypes 2–4 was above 0.8 and significantly higher than that found in phenotype 1 (average proportion = 0.28, p < 0.0001). We next wanted to see if significant differences in bleaching sensitivity existed between our four identified clusters/phenotypes. A one-way ANOVA with a Tukey post hoc found differences in the observed % change in absorbance and Fv/Fm across clusters (p < 0.0001). For Absorbance,

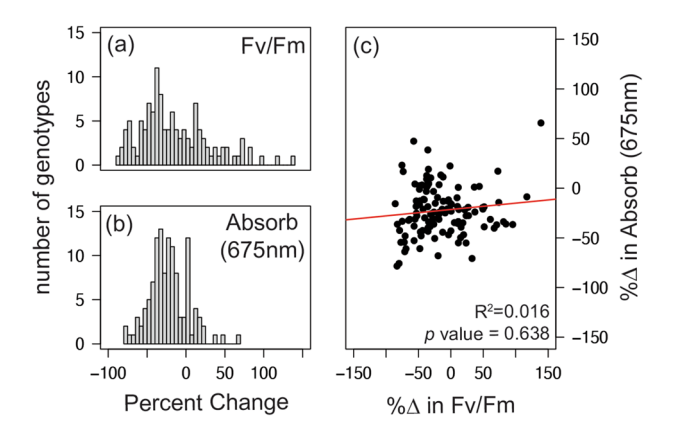


**Fig. 2** Bleaching Response Metrics: Results of the six-week thermal stress experiment were characterized by recording Fv/Fm and Absorbance (at 675 nm) measurements from each coral colony and represented as the percent change between control and high-temperature conditions. Distribution of colony responses are displayed as separate histograms for  $\%\Delta$  in Fv/Fm (a) and  $\%\Delta$  in Absorbance (b). Individual colony responses for both bleaching response metrics are reflected in the correlation plot in panel (c) where the red line represents the best linear fit to the data



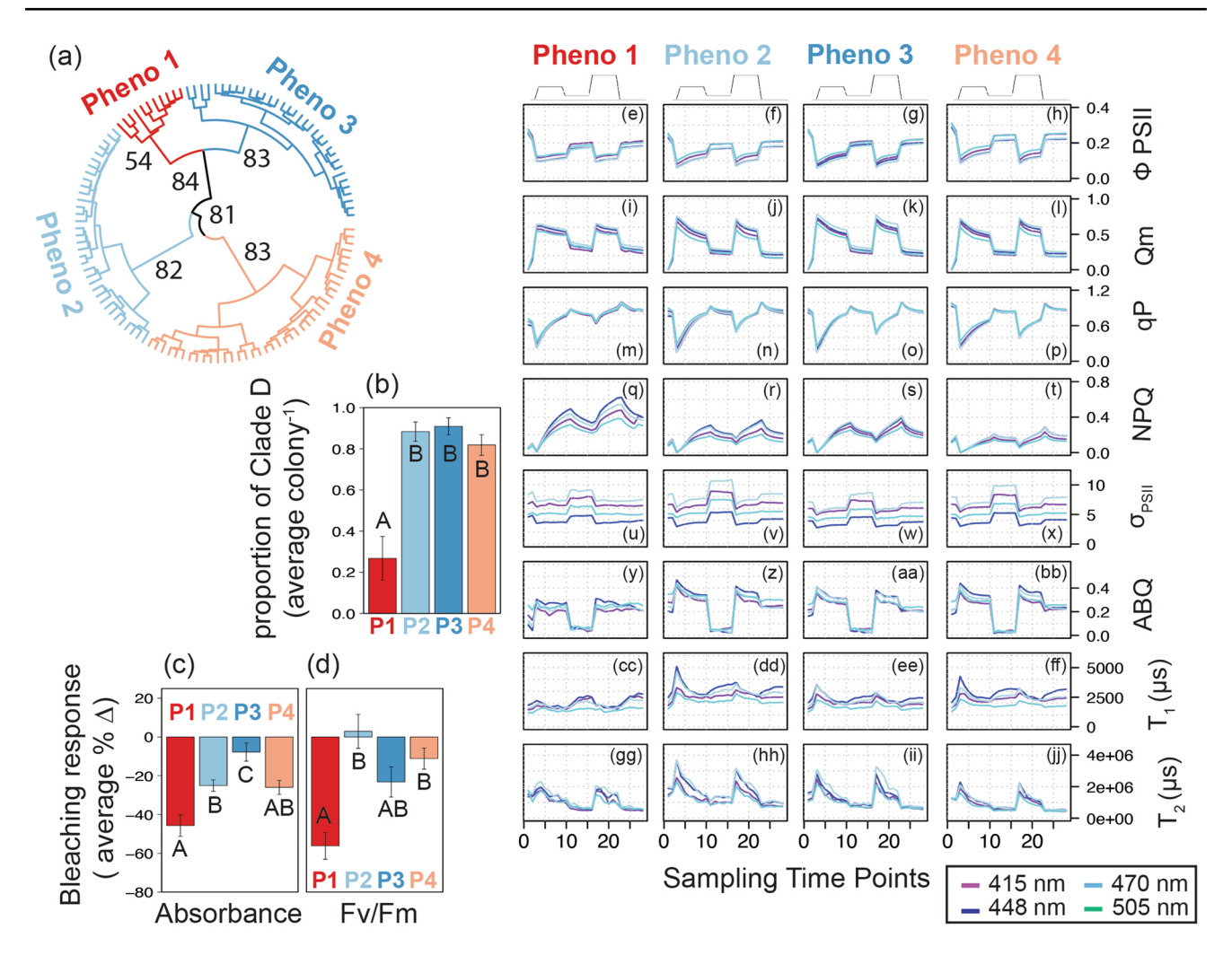


**Fig. 3** Coral Photosymbiont Phenotypic Variability: Phenomic dendrogram (a) derived from 716 photo-physiological metrics (autocorrelation values < 0.99 Rho). The largest four clusters are color coded (a). Bootstrap values are based on 10,000 iterations and are indicated for major nodes delineating the four phenotypes. Middle bar graph reflects the average ± se proportion of clade D symbionts within coral colonies in each cluster (b). Lower bar graphs reflect the average ± se for observed temperature-induced changes in absorbance (c) and Fv/Fm (d) for the four identified clusters/phenotypes from the dendrogram. Letters under individual bars represent significant differences across phenotypes as measured using a one-way ANOVA with a

Tukey post hoc or pairwise Wilcoxon. Mean photo-physiological traces for each identified phenotype are reflected in panels  $\mathbf{e}-\mathbf{j}\mathbf{j}$  where line color indicates excitation wavelength with purple representing 415 nm; dark blue, 448 nm; light blue, 470 nm; and teal blue, 505 nm. The gray line directly above panels  $\mathbf{e}-\mathbf{h}$  displays the variable light protocol. Panels  $\mathbf{e}-\mathbf{h}$  reflect the Quantum Yield of PSII ( $\Phi_{\text{PSII}}$ ),  $\mathbf{i}-\mathbf{l}$  reflects the partial pressure over PSII ( $Q_{\text{m}}$ ),  $\mathbf{m}-\mathbf{p}$  reflects photochemical quenching (qP),  $\mathbf{q}-\mathbf{t}$  reflects non-photochemical quenching (NPQ),  $\mathbf{u}-\mathbf{x}$  reflects the absorption cross section of PSII ( $\sigma_{\text{PSII}}$ ),  $\mathbf{y}-\mathbf{b}\mathbf{b}$  reflects antennae bed quenching,  $\mathbf{cc}-\mathbf{ff}$  and  $\mathbf{gg}-\mathbf{jj}$  reflects the reoxidation constants  $\tau_1^{\text{ST}}$  and  $\tau_2^{\text{ST}}$ , respectively

phenotype 1 displayed a significantly (p < 0.044) larger response to thermal stress as compared to phenotypes 2 and 3 (Fig. 3c). Phenotypes 2 (p = 0.01) and 4 (p = 0.004) also had a significantly larger response to thermal stress as compared to the most resistant phenotype (phenotype3). For high-temperature-induced changes in Fv/Fm, phenotype 1 had a significantly (p < 0.002) larger reduction as compared to phenotypes 2 and 4 (Fig. 3e–h).

#### Contrasting light-response phenotypes

Quantum yield of PSII ( $\Phi_{PSII}$ ) light-response profiles were significantly different as yields in Phenotype 4 were generally higher than those in phenotypes 1, 2 and 3 (p<0.0001, Fig. 3e–h). A minor, although significant, difference in partial pressure over PSII ( $Q_{\rm m}$ ) profiles between phenotype 3 and phenotypes 2 and 4 was also found (p<0.001, Fig. 3i–l). Photochemical quenching response profiles (qP) also differed across phenotypes as initial quenching were



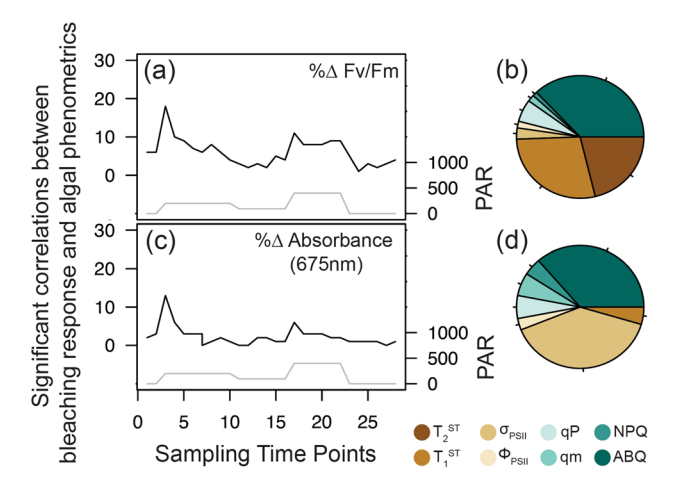


Fig. 4 Phenomic versus Bleaching Response Correlations: A correlation matrix was used to assess relationships between bleaching response metrics ( $\%\Delta$  in Fv/Fm and  $\%\Delta$  in absorbance) and all algal photo-physiological metrics derived from the multispectral single-turnover fluorometer. Panels **a** and **c** reflect significant correlations (spearman) between photo-physiological metrics and  $\%\Delta$  in Fv/Fm or  $\%\Delta$  in absorbance (170 and 66 total/resulting metrics, respectively) and are summarized according to the sampling time point (black line) from which they are derived. The gray line in each figure reflects the PAR values for each step in the actinic light protocol. Pie charts in panels **b** and **d** reflect the fraction of each algal metric significantly correlated with  $\%\Delta$  in Fv/Fm and  $\%\Delta$  in absorbance, respectively

significantly lower in phenotype 4 as compared to all others (p < 0.05, Fig. 3m-p). NPQ response profiles were significantly higher in phenotype 1 as compared to phenotypes 2, 3 and 4 (p < 0.05) while significant differences were also noted for phenotypes 2 and 3 which were also significantly elevated compared to phenotype 4 (p < 0.01, Fig. 3q-t). The functional absorption cross section of PSII was significantly lower in phenotype 3 as compared to all others (p < 0.0001), while differences between phenotypes 2 and 4 were also noted (p = 0.005, Fig. 3u-x). With the exception of phenotypes 3 and 4, significant differences in antennae bed quenching profiles were observed across all phenotypes (p < 0.002, Fig. 3y-bb). Phenotype 2 profiles for Tau 1 and Tau 2 were significantly higher than all other phenotypes (p < 0.005, Fig. 3cc-ji). Tau 1 profiles for phenotype 1 were also significantly lower than phenotype 4 (p < 0.0001) while Tau 2 profiles for phenotype 3 were significantly higher than phenotype 4 (p < 0.0001).

# Correlations between algal phenomics and bleaching response metrics

A total of 896 photo-physiological responses (8 photophysiological responses \* 4 excitation wavelengths \* 28 sampling time points) were measured as part of our photophysiologic-based phenometric assay. Using data from all 120 colonies, these photo-physiological metrics were first screened for high-correlation (Rho > 0.85) with one another and then those remaining (311 photo-physiological metrics) were directly tested for significant correlation (p < 0.05) with the two individual bleaching metrics. Only 66 and 170 photo-physiological metrics were deemed to have significant correlation with % change in Absorbance and Fv/Fm, respectively. The absolute range in Rho for significant metrics was between 0.179 and 0.448 for Absorbance and 0.184-0.455 for Fv/Fm (See Supplemental Tables S1 and S2). Correlations were then plotted as a function of which step in the actinic light protocol the phenometric values were derived (Fig. 4a,c). For both bleaching response metrics, significant correlations are predominantly made with phenometrics derived immediately (within 10 s) after an increase in light intensity (sampling time points 3-5 and 17-19), and strongly suggest these transitional periods contain important photochemical signatures related to how symbionts cope with environmental stress. Next, significant correlations for each bleaching response metric were further evaluated by which photo-physiological metrics they reflect (Fig. 4b,d). The most common photo-physiological metrics significantly correlated with % $\Delta$  in FvFm were  $\tau_1^{ST}$  (28%),  $\tau_2^{ST}$  (21%), and antennae bed quenching (37%) while the most common for  $\%\Delta$  in absorbance were the absorbance cross section of PSII (39%), and Antennae Bed Quenching (36%).

#### Predictive bleaching model evaluation

For both bleaching response metrics, Random Forest-based models were able to generate predictions which were significantly correlated with observed trends in thermal bleaching responses (Fig. 5b,e). Importantly, average bootstrapped correlations between observed and predicted responses improved by incorporating additional coral genotypes for model generation (Fig. 5d,g). However, the bootstrappedaveraged accuracy of predicting changes in Fv/Fm peaked with an  $R^2$  value of 0.42 ( $\pm 0.018$  CI, using 80 colonies for model testing). Accuracy in predicting changes in absorbance peaked at 0.33 ( $\pm$  0.019 CI, using 80 colonies for model testing). While our R<sup>2</sup> plots suggest that model accuracy may have improved with additional colonies used in training, the root mean squared error for both metrics plateaued at roughly 23 and 19 (for Fv/Fm and absorbance, respectively) with at least 60 colonies used for model generation. When used to evaluate the average bleaching response for the topand bottom-ranked corals, model results for changes in Fv/ Fm were between 67 and 71% accurate when at least 60 colonies were used to generate the model whereas results for changes in absorbance peaked between 89 and 91% accurate when using at least 60 colonies for model generation (Fig. 5c,f).



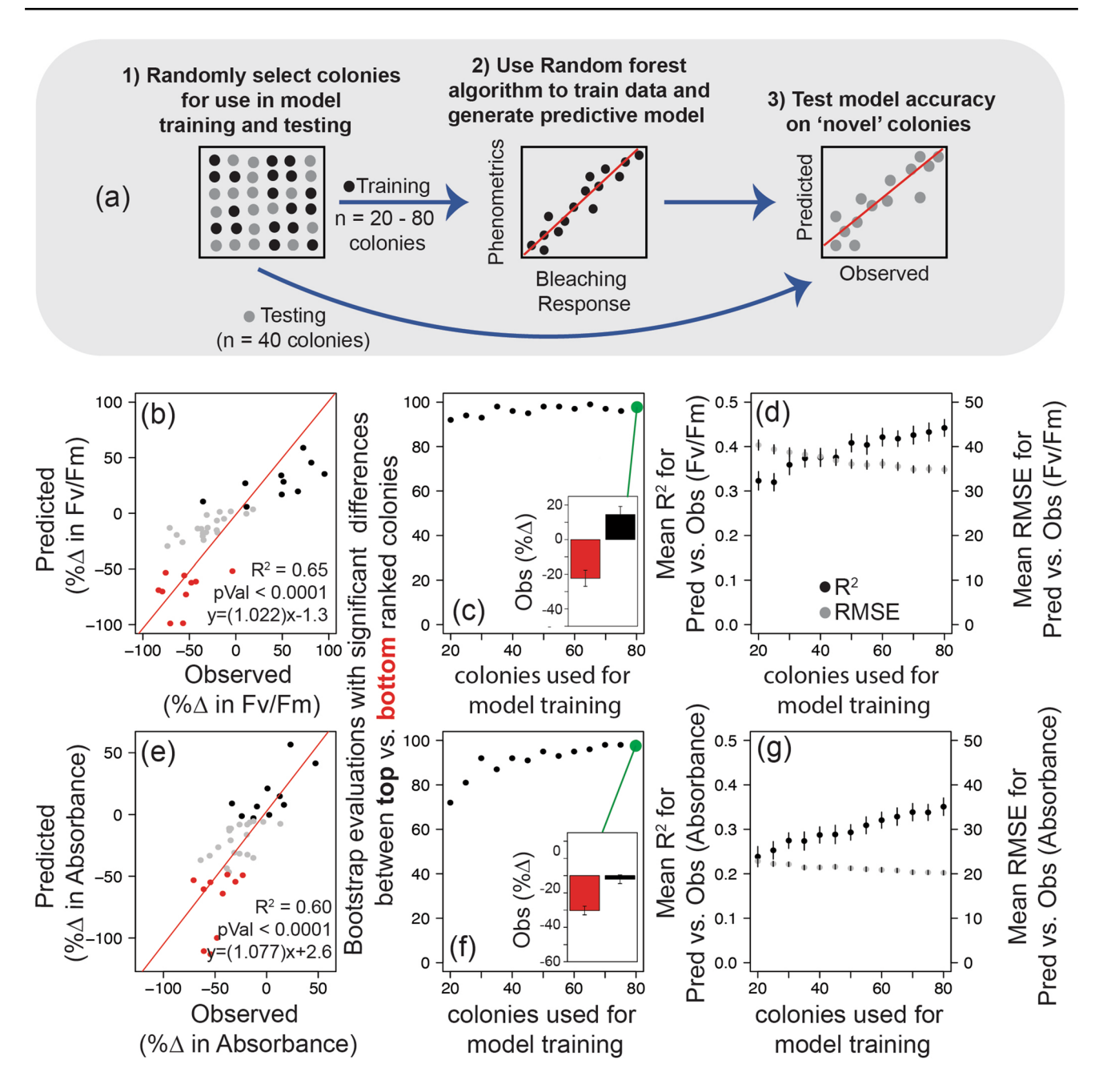


**Fig. 5** Model Training and Evaluation with Bootstrap Resampling: Overall model performance was evaluated based on the total number of colonies utilized in training (between 20 and 80 colonies) while model testing was always carried out using a total of 40 colonies. For each evaluation, samples were randomly selected for training and testing as reflected in panel **a** (steps 1–3). Each evaluation process was bootstrapped 100 times to ensure model outcomes were robust and not reflective of any specific colony sample. Representative test data sets reflecting the Predicted versus Observed bleaching responses as  $\%\Delta$  in Fv/Fm and  $\%\Delta$  in absorbance (675 nm) are found in panels (**b**) and (**e**), respectively. Observed bleaching response scores for the top (black) and bottom (red) ranked samples were then

tested for significant differences using a t test. The number (out of 100) of bootstrapped samples with significant (p < 0.05) differences in observed bleaching scores between the top- and bottom-ranked colonies are reflected in panels  $\mathbf{c}$  (for  $\%\Delta$  in Fv/Fm) and  $\mathbf{f}$  ( $\%\Delta$  in absorbance 675 nm). Inset bar graphs in panels  $\mathbf{c}$  and  $\mathbf{f}$  reflect the mean ( $\pm$ standard deviation) observed bleaching responses for the top- and bottom-ranked colonies as evaluated with a model using 68 colonies for training. Panels  $\mathbf{d}$  and  $\mathbf{g}$  reflect the mean ( $\pm$ 95% CI)  $R^2$  correlation (black dots) and RMSE (gray dots) values between the Observed and Predicted data (as represented in panels  $\mathbf{b}$  and  $\mathbf{e}$ ) as a function of the number of colonies utilized to train each model

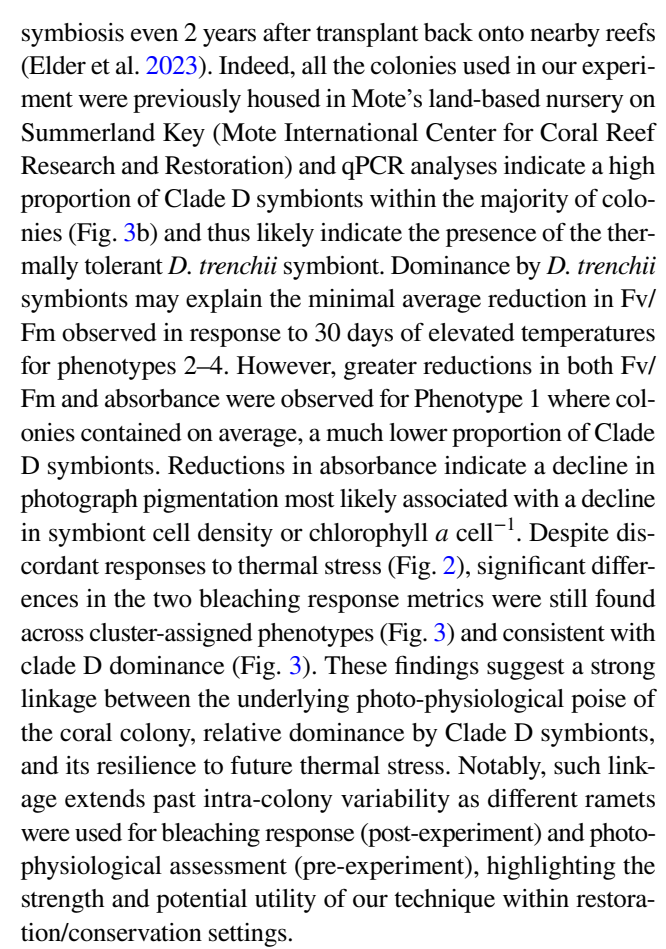


### Discussion

Our objective was to determine if easily measured, chlorophyll-a fluorescence-based photo-physiological metrics could be used as a predictive tool for determining thermal tolerance among different genotypes of the coral Acropora palmata. Identifying the degree of thermal tolerance among different genotypes of the same coral species (or different corals) is a common goal for many field studies and restoration initiatives (Voolstra et al. 2020, 2021; Grummer et al. 2022; Evensen et al. 2023), yet current practices often require labor-intensive experimental procedures, includes sacrificing biomass of critically endangered coral species, and the outcome is limited to only coral genotypes utilized in the study. Establishing an Artificial Intelligence (AI) based approach where non-invasive measurements can be used to predict thermal tolerance in novel colonies could remove a major bottleneck in trait-based identification/selection of reef corals within basic and applied research settings. Despite low correlation between our two bleaching response metrics (Fv/Fm and absorbance, Fig. 2c), our phenomicbased dendrogram indicated that significant differences in bleaching sensitivity existed across identified clusters (Fig. 3a) which appear driven by the underlying symbiont species (Fig. 3b). This correlation suggests that underlying photo-physiological data can be used to forecast thermal response within individual colonies. To test this concept, we trained a Random Forest-based algorithm using algal phenotypic data, along with bleaching response metrics to predict temperature tolerance in novel coral species (Fig. 4, 5). Such an approach can extend results of an experiment using data derived from bleaching assays to train a model to infer information on novel coral genotypes, thereby vastly increasing the value and utility of an individual experiment. High-throughput assays for identification of thermal stress already rely on photochemical signatures to assess holobiont response (Voolstra et al. 2020; Cunning et al. 2021), and our approach builds on these ideas through a massive increase in the quantity and dimensionality of photosynthetic-data available.

#### Phenotypic variability in bleaching response

Bleaching response metrics were evaluated for each coral genotype as a percent change between fragments from control and high-temperature treatments. Percent change in Fv/Fm varied broadly across individual genotypes yet collectively averaged close to zero, indicating relative thermal stability of the symbionts (Fig. 2a). While *A. palmata* colonies in situ are commonly found to host *Symbiodinium fitti* (LaJeunesse 2002), colonies acclimated to MML-IC2R3's land-based nurseries are often dominated by the more thermally tolerant symbiont, *Durusdinium trenchii* (Gantt et al. 2023) and can retain this



Concordant responses in Fv/Fm and absorbance found in prior studies assume that bleaching is the result of thermal damage to the algal photosynthetic apparatus which induces the over-production of radical oxygen species (ROS) which leach out into the host environment and promote the signaling cascade that triggers cell expulsion (bleaching) (Weis 2008; Hawkins and Davy 2012; Hawkins et al. 2015). Indeed, this thermal stress pathway is common among many coral species, especially those considered thermally sensitive (Weis et al. 2008; Weis 2008). However, thermal stress may also reduce ROS scavenging activity by the host (Baird et al. 2009), potentially leading to cell expulsion without any degradation to the photosynthetic apparatus within the symbiont. Such discrepancies can lead to discordant interpretations of bleaching tolerance based on what bleaching response metrics are utilized. Identifying what physiological traits link to these separate responses is thus a critical step toward understanding and predicting discordant patterns of thermal response, such as those observed here.

# Linkage between bleaching response and fluorescent signatures of photosynthetic poise

Standard Photosynthesis to irradiance curve protocols incrementally raise light intensity and monitor photochemical



response to understand light stress and acclimation mechanisms in marine algae (Warner et al. 2010). Typically, each incremental light step is followed by a brief (20 s to 5 min) period to allow for acclimation prior to measuring the photochemical response. However, our protocol continuously records photochemical responses throughout our actinic light protocol, capturing the acclimation phase as well (see Figs. 1 and 3). This unique protocol thus allows for a higherresolution understanding of rapid photochemical changes in response to variable light. Notably, measurement periods immediately after transitioning from dark (or low light) to higher light intensity were most correlated with bleaching response metrics (Fig. 4a,c). Prior studies have highlighted the importance of understanding photochemical responses to quick transitions in light intensity (Allahverdiyeva and Suorsa 2015; Andersson et al. 2019) and variability is indeed notable across species of Symbiodiniaceae (Hoadley et al. 2023). Here, our light-response profiles (Fig. 3e-jj) indicate differences in how each of our phenotypes respond to changes in light. Specifically, initial responses to the onset of actinic light (sampling time point 3) are particularly different for ABQ,  $\tau_1^{ST}$  and  $\tau_2^{ST}$  within the more thermally sensitive of the identified phenotypes (phenotype 1). Better performance via smaller or faster acclimatization to rapid changes in light may serve as a proxy for overall stress mitigation and may explain why these metrics are more correlated with bleaching response as compared with subsequent measurements of each light acclimation step. However, further research that focuses on understanding the phenotypic variability within individual coral species or even across multiple coral and symbiont types will be required to understand if such connections are prevalent across the Symbiodiniaceae family or if the relative importance of individual photo-physiological metrics or acclimatization periods differ across species or environments. Other metrics such as NPQ also appear higher within phenotype 1 and are consistent with previous observations across thermally sensitive and tolerant symbiont types (Hennige et al. 2011; Hoadley et al. 2023).

Correlation matrices identified separate algal phenometrics as providing the best correlations with the two bleaching response metrics (Fv/Fm and absorbance, Fig. 4b–d). Changes in reoxidation kinetics ( $\tau_1^{ST}$  and  $\tau_2^{ST}$ ) represented the largest portion of metrics with a significant correlation to temperature-induced changes in Fv/Fm (Fig. 4b) and describe the rate of electron transport through and the downstream of the PSII reaction center (Schuback et al. 2021). Reoxidation kinetics are often used to identify stress or degradation at different sites that may lower or inhibit photosynthetic capacity (Hoadley et al. 2021, 2023; Suggett et al. 2022) and may explain the relationship with changes in Fv/Fm observed here (Supplemental Figure S2, and Table S1). In contrast, changes in absorbance due to high temperatures were most linked to measurements of the

absorption cross section of PSII which reflects the size of light-harvesting compounds connected to a PSII reaction center. Given this direct connection to photopigments, it is perhaps not surprising that this metric was well correlated with the percent change in absorbance during thermal stress (Fig. 4d, Supplemental Figure S1, and Table S2). Additionally, antennae bed quenching (ABQ) was also well correlated with both bleaching response metrics (absorbance and Fv/Fm) and describes the reorientation of light harvesting pigments to dissipate excess light energy. Changes in ABO may therefor serve as an important proxy for the bleaching response pathway which starts in the symbiont and leads to host driven cell expulsion. Understanding what traits are best utilized to assess thermal response is critical for evaluating the bleaching phenotype and our results here indicate that each response metric has unique sets of biomarkers. However, future use of specific photo-physiological metrics as biomarkers will also need to incorporate seasonal and environmental impacts on photobiology which may alter relationships with bleaching sensitivity. Future studies that test predictive power across seasons could be a logical next step.

### AI-based predictive models for coral thermal resilience

Model-based predictions using genomic data have previously been applied to evaluating the thermal tolerance of individual colonies of the coral A. millepora (Fuller et al. 2020). However, predictive accuracy was low when based solely on host genetics and improved notably once information on environmental conditions and symbiont dominance was included. On a larger spatial scale, survival rates of coral larvae sourced from different locations have been used to predict which reefs along the Great Barrier Reef are most likely to produce thermally tolerant corals (Quigley and van Oppen 2022). Indeed, AI-based predictive models for coral research and restoration are already in use but lack the high-throughput applicability required for scalable recommendations. Here, our predictive pipeline first uses a correlation matrix to prioritize individual algal photo-physiological metrics which are then fed into a Random Forest AI model and converted into predictions of coral bleaching severity, concordant with experimentally produced observations after long-term (4 weeks) exposure to high-temperature stress (Fig. 4 and 5). Although overall average model strength peaked at 0.42 and 0.33 R<sup>2</sup> (for Fv/Fm and absorbance, respectively), the use of additional colonies for initial training would improve accuracy. In addition, our results do not incorporate colonies with the highest thermal sensitivity as those fragments were removed prior to the end of the experiment and we were thus unable to capture their signal. The lack of low tolerance corals within our training dataset may also have impacted the overall strength of our predictive model. Model improvements through better training data,

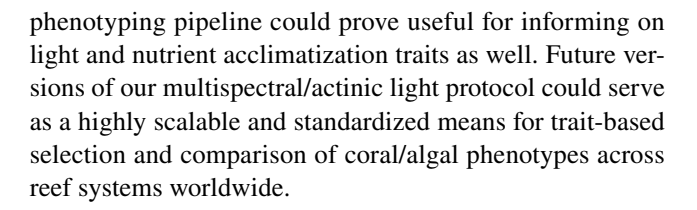


additional colonies or incorporation of additional (easily measured) traits or measurement time points (to capture the thermally sensitive individuals) could help strengthen our approach, providing a robust and broadly applicable technique. Future work will also need to assess prediction accuracy across coral species with and without thermally tolerant symbiont types to assess how discordant responses (Fig. 2) impact overall modeling efforts.

While our method largely focuses on the symbiont photophysiology to make predictions, the coral host's influence on symbiont physiology is well documented as skeletal features, tissue thickness and host-fluorescence proteins all may impact symbiont light acclimation (Enriquez et al. 2005; Enríquez et al. 2017; Wangpraseurt et al. 2017; Xiang et al. 2020; Bollati et al. 2022). Such host-centric physiological variability presumably drives differences in symbiont physiology which can be measured using chlorophyll-a fluorescence techniques (Hoadley et al. 2019). In this context, our technique incorporates direct and indirect metrics of physiology from both the symbiont and host, respectively. However, future predictive techniques that also incorporate additional and direct host-centric physiological metrics such as GFP production or ROS scavenging could further improve predictive accuracy and align with known host genomic traits that infer thermal tolerance (Kenkel et al. 2013a; Dixon et al. 2015; Drury and Lirman 2021; Rose et al. 2021; Quigley and van Oppen 2022).

### Conclusion

By capturing a more complex fluorescent signature that includes rapid responses to varying light using a low cost and open-source instrument, our approach allows for more nuanced photo-physiological differences to be identified and then applied within our modeling pipeline. Tools that increase our capacity to evaluate traits in a highly scalable and accessible fashion are well suited for use toward ongoing coral reef restoration initiatives. Here, chlorophyll-a fluorescence-based algal phenotyping combined with AI predictive models converts our large physiological datasets into actionable products. The relatively low cost of our instrumentation, along with the potential for broad application of trained models, and non-destructive sampling approach, could be highly beneficial as a tool for rapidly selecting coral colonies with desirable traits. Although our focus for this study was thermal tolerance, light, and water quality stress are also common challenges for coral nurseries and outgrowth operations (Vardi et al. 2021; Voolstra et al. 2021) and acclimatization to these stressors is also regulated through a combination of host and symbiont physiology (Hennige et al. 2010; Suggett et al. 2012; Hoadley and Warner 2017; Xiang et al. 2020). Using a similar model training/testing approach, our



Acknowledgements We thank the staff and interns at Mote's International Center for Coral Reef Research and Restoration on Summerland Key, FL for their assistance and support. We thank Sophia Lee, Daniella Leon and Ashley Conde for their help with DNA analyses. Research activities were made possible through the Florida Fish and Wildlife Conservation Commission (SAL-22-2406-SCRP and Florida Keys National Marine Sanctuary (FKNMS-2015-163-A3) permits. The work was funded by the National Science Foundation, grant nos. 2054885 to K.D. Hoadley and the National Ocean and Atmospheric Administration, grant no. NA21NMF4820300 to E.M and C.D.K. The authors declare no competing interests. This project was also supported through the US Naval Research Lab's Base Program.

Author contributions CDK, EM, and CNK planned and designed the thermal bleaching experiment. KH developed the predictive model while GL built the instrument. TK, HE, and CNK collected fragments, setup and conducted the thermal experiments. AM, SL, and SD collected all phenotyping and bleaching response data. HE, SO, and MR extracted DNA and genotyped all samples. KH analyzed the data and wrote the manuscript. All authors provided feedback on the manuscript. KH agrees to serve as the author responsible for contact and ensures communication.

**Data availability** All data needed to evaluate the conclusions in the paper are present in the paper and/or the Supplementary Materials. Raw data and analytical scripts for Figs. 2, 3, 4 and 5 are available via github (khoadley/bleaching-prediction-2023).

### References

Abrego D, Ulstrup KE, Willis BL, van Oppen MJ (2008) Speciesspecific interactions between algal endosymbionts and coral hosts define their bleaching response to heat and light stress. Proc Biol Sci 275:2273–2282

Allahverdiyeva Y, Suorsa M, Tikkanen M, Aro EM (2015) Photoprotection of photosystems in fluctuating light intensities. J Exp Bot 66(9):2427–2436

Andersson B, Shen C, Cantrell M, Dandy DS, Peers G (2019) The fluctuating cell-specific light environment and its effects on cyanobacterial physiology. Plant Physiol 181(2):547–564

Baird AH, Bhagooli R, Ralph PJ, Takahashi S (2009) Coral bleaching: the role of the host. Trends Ecol Evol 24:16–20

Barshis DJ, Birkeland C, Toonen RJ, Gates RD, Stillman JH (2018) High-frequency temperature variability mirrors fixed differences in thermal limits of the massive coral Porites lobata. J Exp Biol 221:jeb188581

Bollati E, Lyndby NH, D'Angelo C, Kühl M, Wiedenmann J, Wangpraseurt D (2022) Green fluorescent protein-like pigments optimize the internal light environment in symbiotic reef building corals. Elife 11:e73521

Boström-Einarsson L, Babcock RC, Bayraktarov E, Ceccarelli D, Cook N, Ferse SCA, Hancock B, Harrison P, Hein M, Shaver E (2020)



Coral restoration—a systematic review of current methods, successes, failures and future directions. PLoS ONE 15:e0226631

- Caruso C, Hughes K, Drury C (2021) Selecting heat-tolerant corals for proactive reef restoration. Front Mar Sci 8:632027
- Cunning R, Baker AC (2013) Excess algal symbionts increase the susceptibility of reef corals to bleaching. Nat Clim Chang 3:259–262
- Cunning R, Parker KE, Johnson-Sapp K, Karp RF, Wen AD, Williamson OM, Bartels E, D'Alessandro M, Gilliam DS, Hanson G (2021) Census of heat tolerance among Florida's threatened staghorn corals finds resilient individuals throughout existing nursery populations. Proc R Soc B 288:20211613
- Cunning R, Ritson-Williams R, Gates RD (2016) Patterns of bleaching and recovery of Montipora capitata in Kāne 'ohe Bay, Hawai 'i, USA. Mar Ecol Prog Ser 551:131–139
- Dixon GB, Davies SW, Aglyamova GV, Meyer E, Bay LK, Matz MV (2015) Genomic determinants of coral heat tolerance across latitudes. Science 348:1460–1462
- Drury C, Lirman D (2021) Genotype by environment interactions in coral bleaching. Proc R Soc B 288:202010177
- Elder H, Million WC, Bartels E, Krediet CJ, Muller EM, Kenkel CD (2023) Long-term maintenance of a heterologous symbiont association in Acropora palmata on natural reefs. ISME J 17:486–489
- Enriquez S, Mendez ER, Iglesias-Prieto R (2005) Multiple scattering on corals enhances light absorption by symbiotic algae. Limnol Oceanogr 50:1025–1032
- Enríquez S, Méndez ER, Hoegh-Guldberg O, Iglesias-Prieto R (2017) Key functional role of the optical properties of coral skeletons in coral ecology and evolution. Proc R Soc B Biol Sci 284:20161667
- Evans MR, Norris KJ, Benton TG (2012) Predictive ecology: systems approaches. Philos Trans R Soc B Biol Sci 367:163–169
- Evensen NR, Parker KE, Oliver TA, Palumbi SR, Logan CA, Ryan JS, Klepac CN, Perna G, Warner ME, Voolstra CR (2023) The coral bleaching automated stress system (CBASS): a low-cost, portable system for standardized empirical assessments of coral thermal limits. Limnol Oceanogr Methods
- Fuller ZL, Mocellin VJL, Morris LA, Cantin N (2020) Population genetics of the coral <i>Acropora millepora</i>: toward genomic prediction of bleaching. Science
- Galili T (2015) dendextend: an R package for visualizing, adjusting and comparing trees of hierarchical clustering. Bioinformatics 31:3718–3720
- Gantt SE, Keister EF, Manfroy AA, Merck DE, Fitt WK, Muller EM, Kemp DW (2023) Wild and nursery-raised corals: comparative physiology of two framework coral species. Coral Reefs 42:299–310
- Grummer JA, Booker TR, Matthey-Doret R, Nietlisbach P, Thomaz AT, Whitlock MC (2022) The immediate costs and long-term benefits of assisted gene flow in large populations. Conserv Biol 36:e13911
- Hawkins TD, Davy SK (2012) Nitric oxide production and tolerance differ among Symbiodinium types exposed to heat stress. Plant Cell Physiol 53:1889–1898
- Hawkins TD, Krueger T, Wilkinson SP, Fisher PL, Davy SK (2015) Antioxidant responses to heat and light stress differ with habitat in a common reef coral. Coral Reefs. https://doi.org/10.1007// s00338-015
- Hennige SJ, Smith DJ, Walsh S-J, McGinley MP, Warner ME, Suggett DJ (2010) Acclimation and adaptation of scleractinian coral communities along environmental gradients within an Indonesian reef system. J Exp Mar Biol Ecol 391:143–152
- Hennige SJ, McGinley MP, Grottoli AG, Warner ME (2011) Photoinhibition of *Symbiodinium* spp. within the reef corals *Montastraea faveolata* and *Porites astreoides*: implications for coral bleaching. Mar Biol 158:2515–2526
- Hoadley KD, Lewis AM, Wham DC, Pettay DT, Grasso C, Smith R, Kemp DW, LaJeunesse TC, Warner ME (2019) Host-symbiont

- combinations dictate the photo-physiological response of reefbuilding corals to thermal stress. Sci Rep 9:9985
- Hoadley KD, Warner ME (2017) Use of open source hardware and software platforms to quantify spectrally dependent differences in photochemical efficiency and functional absorption cross section. Front Mar Sci. https://doi.org/10.3389/fmars.2017.00365
- Hoadley KD, Lockridge G, McQuagge A, Pahl KB, Lowry S, Wong S, Craig Z, Petrik C, Klepac C, Muller EM (2023) A phenomic modeling approach for using chlorophyll-a fluorescence-based measurements on coral photosymbionts. Front Mar Sci 10:1092202
- Hoadley KD, Pettay DT, Dodge D, Warner ME (2016) Contrasting physiological plasticity in response to environmental stress within different chidarians and their respective symbionts. Coral Reefs 35:1–14
- Hoadley KD, Pettay DT, Lewis A, Wham D, Grasso C, Smith R, Kemp DW, LaJeunesse T, Warner ME (2021) Different functional traits among closely related algal symbionts dictate stress endurance for vital Indo-Pacific reef-building corals. Glob Chang Biol 27:5295–5309
- Hothorn T, Bretz F, Westfall P (2008) Simultaneous inference in general parametric models. Biom J J Math Methods Biosci 50:346–363
- Hughes TP, Anderson KD, Connolly SR, Heron SF, Kerry JT, Lough JM, Baird AH, Baum JK, Berumen ML, Bridge TC (2018) Spatial and temporal patterns of mass bleaching of corals in the Anthropocene. Science 359:80–83
- Hughes TP, Kerry JT, Álvarez-Noriega M, Álvarez-Romero JG, Anderson KD, Baird AH, Babcock RC, Beger M, Bellwood DR, Berkelmans R (2017) Global warming and recurrent mass bleaching of corals. Nature 543:373
- Iglesias-Prieto R, Beltran VH, LaJeunesse TC, Reyes-Bonilla H, Thome PE (2004) Different algal symbionts explain the vertical distribution of dominant reef corals in the eastern Pacific. Proc R Soc London Ser B Biol Sci 271:1757–1763
- Kenkel CD, Goodbody Gringley G, Caillaud D, Davies SW, Bartels E, Matz MV (2013a) Evidence for a host role in thermotolerance divergence between populations of the mustard hill coral (Porites astreoides) from different reef environments. Mol Ecol 22:4335–4348
- Kenkel CD, Matz MV (2016) Gene expression plasticity as a mechanism of coral adaptation to a variable environment. Nat Ecol Evol 1:14
- Kenkel CD, Meyer E, Matz MV (2013b) Gene expression under chronic heat stress in populations of the mustard hill coral (*Porites astreoides*) from different thermal environments. Mol Ecol 22:4322–4334
- Kitchen SA, Von Kuster G, Kuntz KLV, Reich HG, Miller W, Griffin S, Fogarty ND, Baums IB (2020) STAGdb: a 30K SNP genotyping array and Science Gateway for Acropora corals and their dinoflagellate symbionts. Sci Rep 10:12488
- Klepac CN, Eaton KR, Petrik CG, Arick LN, Hall ER, Muller EM (2023) Symbiont composition and coral genotype determines massive coral species performance under end-of-century climate scenarios. Front Mar Sci 10:1026426
- Kolber Z, Prasil O, Falkowski P (1998) Measurements of variable chlorophyll fluorescence using fast repetition rate techniques: defining methodology and experimental protocols. Biochimica Et Biophysica Acta (BBA) Bioenergetics 1367:88–107
- Kursa MB, Rudnicki WR (2010) Feature selection with the Boruta package. J Stat Softw 36:1–13
- Kuznetsova A, Brockhoff PB, Rune H, Christensen B (2017) ImerTest package: tests in linear mixed effects models. J Stat Softw. https:// doi.org/10.18637/jss.v082.i13
- LaJeunesse T (2002) Community structure and diversity of symbiotic dinoflagellate populations from a Caribbean coral reef. Mar Biol 141:387–400



- LaJeunesse TC, Parkinson JE, Gabrielson PW, Jeong HJ, Reimer JD, Voolstra CR, Santos SR (2018) Systematic revision of Symbiodiniaceae highlights the antiquity and diversity of coral endosymbionts. Curr Biol 28(2570–2580):e6
- McQuagge A, Pahl KB, Wong S, Melman T, Linn L, Lowry S, Hoadley KD (2023) Cellular traits regulate fluorescencebased light-response phenotypes of coral photosymbionts living in-hospite. Front Physiol 14:1244060. https://doi.org/10.3389/fphys.2023. 1244060
- Oxborough K, Moore CM, Suggett DJ, Lawson T, Chan HG, Geider RJ (2012) Direct estimation of functional PSII reaction center concentration and PSII electron flux on a volume basis: a new approach to the analysis of Fast Repetition Rate fluorometry (FRRf) data. Limnol Oceanogr Methods 10(3):142–154
- Palacio-Castro AM, Dennison CE, Rosales SM, Baker AC (2021) Variation in susceptibility among three Caribbean coral species and their algal symbionts indicates the threatened staghorn coral, Acropora cervicornis, is particularly susceptible to elevated nutrients and heat stress. Coral Reefs 40:1601–1613
- Palumbi SR, Barshis DJ, Traylor-Knowles N, Bay RA (2014) Mechanisms of reef coral resistance to future climate change. Science 344:895–898
- Parkinson JE, Baker AC, Baums IB, Davies SW, Grottoli AG, Kitchen SA, Matz MV, Miller MW, Shantz AA, Kenkel CD (2020) Molecular tools for coral reef restoration: beyond biomarker discovery. Conserv Lett 13:e12687
- Parkinson JE, Banaszak AT, Altman NS, LaJeunesse TC, Baums IB (2015) Intraspecific diversity among partners drives functional variation in coral symbioses. Sci Rep 5:15667
- Quigley KM, van Oppen MJH (2022) Predictive models for the selection of thermally tolerant corals based on offspring survival. Nat Commun 13:1543
- Reichstein M, Camps-Valls G, Stevens B, Jung M, Denzler J, Carvalhais N (2019) Deep learning and process understanding for datadriven Earth system science. Nature 566:195–204
- Rodriguez-Román A, Hernández-Pech X, Thomé PE, Enriquez S, Iglesias-Prieto R (2006) Photosynthesis and light utilization in the Caribbean coral *Montastraea faveolata* recovering from a bleaching event. Limnol Oceanogr 51:2702–2710
- Rose NH, Bay RA, Morikawa MK, Thomas L, Sheets EA, Palumbi SR (2021) Genomic analysis of distinct bleaching tolerances among cryptic coral species. Proc R Soc B 288(1960):20210678
- Schuback N, Tortell PD, Berman-Frank I, Campbell DA, Ciotti A, Courtecuisse E, Erickson ZK, Fujiki T, Halsey K, Hickman AE (2021) Single-turnover variable chlorophyll fluorescence as a tool for assessing phytoplankton photosynthesis and primary productivity: opportunities, caveats and recommendations. Front Mar Sci 8:690607
- Suggett DJ, Goyen S, Evenhuis C, Szabó M, Pettay DT, Warner ME, Ralph PJ (2015) Functional diversity of photobiological traits within the genus Symbiodinium appears to be governed by the interaction of cell size with cladal designation. New Phytol 208:370–381
- Suggett DJ, Dong LF, Lawson T, Lawrenz E, Torres L, Smith DJ (2012) Light availability determines susceptibility of reef building corals to ocean acidification. Coral Reefs 32:327–337
- Suggett DJ, Nitschke MR, Hughes DJ, Bartels N, Camp EF, Dilernia N, Warner ME (2022) Toward bio-optical phenotyping of

- reef-forming corals using light-induced fluorescence transientfast repetition rate fluorometry. Limnol Oceanogr Methods 20(3):172–191
- Suggett DJ, Warner ME, Leggat W (2017) Symbiotic dinoflagellate functional diversity mediates coral survival under ecological crisis. Trends Ecol Evol 32:735–745
- Suzuki R, Shimodaira H (2013) Hierarchical clustering with *P*-values via multiscale bootstrap resampling. R package
- Team RC (2017) R: a language and environment for statistical computing. R Foundation for Statistical Computing, Vienna. https://www.R-project.org
- van Woesik R, Shlesinger T, Grottoli AG, Toonen RJ, Vega Thurber R, Warner ME, Marie Hulver A, Chapron L, McLachlan RH, Albright R (2022) Coral-bleaching responses to climate change across biological scales. Glob Chang Biol 28:4229–4250
- Vardi T, Hoot WC, Levy J, Shaver E, Winters RS, Banaszak AT, Baums IB, Chamberland VF, Cook N, Gulko D (2021) Six priorities to advance the science and practice of coral reef restoration worldwide. Restor Ecol 29:e13498
- Voolstra CR, Buitrago-López C, Perna G, Cárdenas A, Hume BCC, Rädecker N, Barshis DJ (2020) Standardized short-term acute heat stress assays resolve historical differences in coral thermotolerance across microhabitat reef sites. Glob Chang Biol 26:4328–4343
- Voolstra CR, Suggett DJ, Peixoto RS, Parkinson JE, Quigley KM, Silveira CB, Sweet M, Muller EM, Barshis DJ, Bourne DG (2021) Extending the natural adaptive capacity of coral holobionts. Nat Rev Earth Environ 2:747–762
- Wangpraseurt D, Holm JB, Larkum AWD, Pernice M, Ralph PJ, Suggett DJ, Kühl M (2017) In vivo microscale measurements of light and photosynthesis during coral bleaching: evidence for the optical feedback loop. Front Microbiol 8:59
- Warner M, Fitt W, Schmidt G (1999) Damage to photosystem II in symbiotic dinoflagellates: a determinant of coral bleaching. Proc Natl Acad Sci USA 96:8007–8012
- Warner ME, Ralph PJ, Lesser MP (2010) Chlorophyll fluorescence in reef building corals. In: Chlorophyll fluorescence in aquatic sciences: methods and applications, Suggett DJ, Prasil O, Borowitzka M, eds. Springer), pp 500
- Weis VM, Davy SK, Hoegh-Guldberg O, Rodriguez-Lanetty M, Pringle JR (2008) Cell biology in model systems as the key to understanding corals. Trends Ecol Evol 23:369–376
- Weis VM (2008) Cellular mechanisms of Cnidarian bleaching: stress causes the collapse of symbiosis. J Exp Biol 211:3059–3066
- Xiang T, Lehnert E, Jinkerson RE, Clowez S, Kim RG, DeNofrio JC, Pringle JR, Grossman AR (2020) Symbiont population control by host-symbiont metabolic interaction in Symbiodiniaceae-cnidarian associations. Nat Commun 11:1–9
- **Publisher's Note** Springer Nature remains neutral with regard to jurisdictional claims in published maps and institutional affiliations.
- Springer Nature or its licensor (e.g. a society or other partner) holds exclusive rights to this article under a publishing agreement with the author(s) or other rightsholder(s); author self-archiving of the accepted manuscript version of this article is solely governed by the terms of such publishing agreement and applicable law.

